Development of an enzyme-linked immunosorbent assay for detection of cellular and in vivo LRRK2 S935 phosphorylation

Published in:
Journal of Pharmaceutical and Biomedical Analysis

Publication status and date:
Published: 25/03/2013

DOI (link to publisher):
10.1016/j.jpba.2012.12.002

Document Version
Publisher's PDF, also known as Version of record

Journal of Pharmaceutical and Biomedical Analysis 76 (2013) 49–58

Contents lists available at SciVerse ScienceDirect

Journal of Pharmaceutical and Biomedical Analysis

journal homepage: www.elsevier.com/locate/jpba

Development of an enzyme-linked immunosorbent assay for detection of cellular and *in vivo* LRRK2 S935 phosphorylation

Lore Delbroek[a], Kristof Van Kolen[a,*], Liesbeth Steegmans[a], Raquel da Cunha[b,c], Wim Mandemakers[b,c], Guy Daneels[a], Pieter-Jan De Bock[d,e], Jinwei Zhang[f], Kris Gevaert[d,e], Bart De Strooper[b,c], Dario R. Alessi[f], Patrik Verstreken[b,c], Diederik W. Moechars[a]

[a] *Janssen Pharmaceutical Companies of Johnson and Johnson, Department of CNS Research, Turnhoutseweg30, 2340 Beerse, Belgium*
[b] *VIB Center for the Biology of Disease, Herestraat 49, 3000 Leuven, Belgium*
[c] *KU Leuven, Center for Human Genetics and Leuven Research Institute for Neuroscience and Disease (LIND), Herestraat 49, 3000 Leuven, Belgium*
[d] *VIB, Department of Medical Protein Research, A. Baertsoenkaai 3, 9000 Ghent, Belgium*
[e] *Ghent University, Department of Biochemistry, 9000 Ghent, Belgium*
[f] *MRC Protein Phosphorylation Unit, University of Dundee, College of Life Sciences, The Sir James Black Centre, Dow Street, Dundee DD1 5EH, Scotland, UK*

ARTICLE INFO

Article history:
Received 1 October 2012
Received in revised form
29 November 2012
Accepted 4 December 2012
Available online 16 December 2012

Keywords:
LRRK2
ELISA
S935 phosphorylation
Parkinson's disease

ABSTRACT

After the discovery of kinase activating mutations in leucine-rich repeat kinase 2 (LRRK2) as associated with autosomal dominant forms of Parkinson's disease, inhibition of the kinase is being extensively explored as a disease modifying strategy. As signaling properties and substrate(s) of LRRK2 are poorly documented, autophosphorylation has been an important readout for the enzyme's activity. Western blotting using anti-phospho-S910 or S935 LRRK2 antibodies showed effectiveness in demonstrating inhibitory effects of compounds.

In this communication we describe two types of enzyme-linked immunosorbent assays (ELISA) to determine LRRK2 protein levels and kinase activity. Both assays take advantage of the sensitivity of the earlier described total and pS935 antibodies for detection (Nichols et al., Biochem. J. 2010) [10]. The first assay is based on anti-GFP-based capturing of overexpressed LRRK2 and is highly suitable to show cellular effects of kinase inhibitors in a 96-well format. In the other platform anti-LRRK2-based capturing allows detection of endogenously expressed LRRK2 in rat tissue with no significant signal in tissue from LRRK2 knockout rats. Furthermore, both assays showed a significant reduction in pS935 levels on cellular and transgenic R1441C/G LRRK2. With the anti-LRRK2 ELISA we were able to detect LRRK2 phosphorylation in human peripheral blood mononuclear cells (PBMC).

To conclude, we report two sensitive assays to monitor LRRK2 expression and kinase activity in samples coming from cellular and *in vivo* experimental settings. Both can show their value in drug screening and biomarker development but will also be useful in the elucidation of LRRK2-mediated signaling pathways.

Abbreviations: LRRK2, leucine-rich repeat kinase 2; PD, Parkinson's disease; S910/935, serine 910/935; HEK293, human embryonic kidney 293; FCS, fetal calf serum; PBMC, peripheral blood mononuclear cell; HRP, horseradish-peroxidase; LC–MS/MS, liquid chromatography mass spectrometry; TMB, 3,3′,5,5′-tetramethylbenzidine; MOI, multiplicity of infection; ELISA, enzyme-linked immunosorbent assay; WT, wildtype; KO, knockout; Tg, transgenic; NT, non-transgenic.

* Corresponding author. Tel.: +32 014 605275.
E-mail addresses: ldelbroe@its.jnj.com (L. Delbroek), kvkolen@its.jnj.com (K. Van Kolen), lsteegm@its.jnj.com (L. Steegmans), raquel.dacunha@cme.vib-kuleuven.be (R. da Cunha), wim.mandemakers@cme.vib-kuleuven.be (W. Mandemakers), gdaneels@its.jnj.com (G. Daneels), pieterj.debock@ugent.be (P.-J. De Bock), j.c.zhang@dundee.ac.uk (J. Zhang), kris.gevaert@ugent.be (K. Gevaert), bart.destrooper@cme.vib-kuleuven.be (B. De Strooper), d.r.alessi@dundee.ac.uk (D.R. Alessi), patrik.verstreken@cme.vib-kuleven.be (P. Verstreken), dmoechar@its.jnj.com (D.W. Moechars).

0731-7085/$ – see front matter © 2012 Elsevier B.V. All rights reserved.
http://dx.doi.org/10.1016/j.jpba.2012.12.002

1. Introduction

Parkinson's disease (PD) is one of the main neurodegenerative diseases causing motor impairment, associated with progressive loss of dopaminergic neurons in midbrain regions *e.g. substantia nigra pars compacta*, and non-motor symptoms like depression, anxiety and deficits in olfactory function. The latter non-motor symptoms have been suggested to be unrelated to impaired dopaminergic transmission. Although the majority of PD cases are thought to be sporadic and caused by a combination of aging and environmental factors, several gene loci have been associated with familial PD [1]. One of these loci is the *PARK8* locus, which harbors a gene encoding for leucine-rich repeat kinase 2 (LRRK2). Mutations in LRRK2, a large (286 kDa) multidomain protein, are linked to autosomal dominant forms of PD. In particular the G2019S mutation, that causes increased kinase activity, has been demonstrated to be responsible for 4% of familial PD cases worldwide. Strikingly, this mutation was also identified in 1% of sporadic PD cases [2,3].

Despite the apparent clinical association between LRRK2 mutations and PD, insight in the underlying mechanism of how these mutations lead to disease progression is limited. One attractive hypothesis is a toxic gain of function of LRRK2 in pathogenesis. This is supported by the observation that several LRRK2 variants show elevated kinase activity. Again, the most striking effects have been noticed for the G2019S mutant. There is less uniformity about the effects of R1441C/G, I2020T and Y1699C variants, as reviewed elsewhere [4]. In addition, the haplotype N551K-R1398H, of which the R1398H mutation has been proposed to reduce kinase activity *in vitro* [5], has been demonstrated to be a protective allele. All these observations suggest that targeting LRRK2 kinase activity is a promising disease modifying approach for treatment of PD. Accordingly, biochemical, cellular and *in vivo* assays to monitor kinase activity of LRRK2 are essential to demonstrate target engagement of compounds. Furthermore, these assays can be used to identify upstream and downstream events in LRRK2-mediated signal transduction, which is essential to gain further insight in the physiological function of LRRK2 kinase activity.

For kinases different concepts of assays have been used successfully. In general these can be divided in three main groups, *i.e.* autophosphorylation, substrate phosphorylation and phenotypic readouts. For LRRK2 several autophosphorylation sites [6] and substrates have been proposed in the literature [7–9]. Whether these can be used to develop relevant assays depends on the availability of sensitive and selective phospho-specific antibodies.

To date, the only antibodies that have been used successfully to monitor cellular LRRK2 kinase activity in crude lysate have been directed towards phosphorylation at S910 and S935 residues [10]. Although these sites are not considered as genuine autophosphorylation sites, inhibition of LRRK2 kinase activity has been shown to downregulate their phosphorylation [11]. This suggests that while these sites might not be autophosphorylation sites LRRK2 activity has a role in their phosphorylation, possibly through the regulation of a feedback pathway involving other kinases.

In this communication we report the development of a high throughput ELISA that can be used to monitor S935 phosphorylation in cells overexpressing GFP-LRRK2 and another one for endogenous levels of total and pS935 LRRK2 in biological samples. Use of the latter demonstrated LRRK2 phosphorylation in different organs derived from rat and a significant reduction of phosphorylation in the pathological R1441C/G mutant in cells and *in vivo*. LRRK2 phosphorylation in peripheral mononuclear blood cells (PBMC) was also demonstrated using this assay.

2. Materials and methods

2.1. Materials

Tissue-culture reagents and BacMam constructs were from Life Technologies. RIPA buffer from Sigma, with added PhosSTOP phosphatase and Complete MINI protease inhibitors (Roche), was used as lysis buffer. Capturing antibodies for ELISA were obtained from Covance (anti-LRRK2) or R&D systems (anti-GFP), antibodies used for detection were kindly provided by Dr. Dario Alessi. Antibodies for immunoprecipitation were from Covance (anti-LRRK2) or Sigma (anti-GFP). For western blotting the antibodies provided by Dr. Alessi were used as primary antibodies, unless indicated otherwise. LRRK2 inhibitor LRRK2-IN-1 was from Calbiochem.

2.2. Animals

Male wildtype and LRRK2 knock-out Long Evans rats (SAGE laboratories) were housed in a pathogen-free facility and exposed to a 12 h light/dark cycle with food and water provided *ad libitum*. At 9 months of age rats were sacrificed by decapitation. Lung, spleen, kidney and brain tissue were removed and immediately snap-frozen in liquid nitrogen. Tissues were homogenized on ice in homogenization buffer (50 mM Tris–HCl pH 7.5, 1 mM EGTA, 1 mM EDTA, 1 mM sodium orthovanadate, 10 mM sodium β-glycerophosphate, 50 mM NaF, 5 mM sodium pyrophosphate, 0.27 M sucrose, 1 mM benzamidine, 2 mM PMSF and 1% Triton X-100 with added phosphatase and protease inhibitors for immunoprecipitation and lysis buffer for ELISA) using a douncer rotating at 600 rpm. The homogenate was centrifugated 15 min at 4 °C at 14,000 rpm. The pellet was discarded and the protein concentration was determined using the BCA method (Thermo Scientific) with BSA as the standard.

The pharmacodynamic study was conducted as described previously [12]. HG-10-102-01 was dissolved in 10% 1-methyl-2-pyrrolidinone (NMP)/90% PEG 300 (Sigma) solution and administered by intraperitoneal injection into wild type male C57BL/6 mice at doses of 0, 10, 30, 50 and 100 mg/kg for 1 h. Control mice were treated with an equal volume of NMP/PEG solution. At the end of treatment, mice were sacrificed by cervical dislocation. Spleen, kidney and brain tissues were rapidly dissected and snap-frozen in liquid nitrogen. Tissues were homogenized in the above-described buffer for immunoprecipitation. Animal experiments were approved by the University of Dundee Ethics Committee and performed under a U.K. Home office project license.

2.3. Cell culture and transfections

HEK293 (human embryonic kidney) cells were cultured in DMEM (Dulbecco's modified Eagle's medium) supplemented with 10% FCS (fetal calf serum), 5×10^6 IU/L penicillin, 5 g/L streptomycin sulphate, 5.5 g/L pyruvic acid and 14.6 g/L L-glutamine. Transduction of cells with GFP-LRRK2 constructs was performed by using the BacMam method (Life Technologies) according to the manufacturer's instructions. Briefly, cells grown to 70–80% confluency were trypsinized and resuspended in full medium at a density of 500,000 cells per 0.5 ml. Subsequently, an equal amount of medium containing BacMam (GFP-LRRK2 or GFP) and enhancer solution was added and the complete suspension was plated in a 9.6 cm^2 dish. After 4 h, medium was replaced by regular cell culture medium. For transduction in a 96-well plate a similar procedure was followed. For transfections with plasmids, Lipofectamine 2000 (Life Technologies) was used according to the manufacturer's instructions. For analysis cells were washed twice with ice-cold PBS, lysed *in situ* with 400 μl lysis buffer, on ice, and centrifugated at 10,000 × *g* at

4 °C for 10 min. Pellets were discarded and protein concentrations were determined using the BCA method.

PBMC are isolated from blood of healthy volunteers. Fifty milliliter freshly isolated blood is diluted in 100 ml PBS. From this suspension, aliquots of 25 ml are transferred to sterile 50 ml tubes, prefilled with 15 ml Lymphoprep (Fresenius Kabi). After centrifugation (20 min, 2000 rpm) the cloudy interface containing PBMC from 2 tubes is pooled and diluted in wash buffer [PBS containing 0.5% human AB serum (PAA, GE Healthcare)] to a volume of 50 ml. The suspension is centrifuged 1 time (10 min, 1200 rpm) and a second time (10 min, 1200 rpm). After the latter, pellets are resuspended in 50 ml wash buffer and counted. After a third centrifugation (10 min, 1200 rpm), the pellet is suspended in MEM/EBSS (Hyclone) and plated into 6 well plates. After incubation (37 °C, 5% CO_2, humidified incubator) overnight, cells are treated with compounds or vehicle during 1 h, centrifuged (1200 rpm, 10 min) and resuspended in ice-cold PBS. After a final centrifugation, cells are lysed in RIPA in the presence of protease and phosphatase inhibitors and analyzed with western blotting or ELISA.

2.4. Western blotting

Cell lysates were resolved by electrophoresis on 4–12% NuPage gradient gels and electroblotted to nitrocellulose membranes. Membranes were blocked with 5% (w/v) skimmed milk in TBST (Tris-buffered saline with Tween-20: 50 mM Tris–HCl, pH 8.0, 0.15 M NaCl and 0.1% (v/v) Tween-20) at room temperature. Membranes were incubated with primary antibody overnight at 4 °C. Primary antibody was used at a concentration of 1 μg/ml, diluted in TBST or 5% bovine albumin serum in TBST. Detection of immune complexes was performed using horseradish-peroxidase (HRP)-conjugated secondary antibodies (GE Healthcare) at a concentration of 1 μg/ml and an enhanced chemiluminescent reagent (West-Femto, Thermo Scientific).

2.5. Immunoprecipitation and mass spectrometry

For immunoprecipitation, the primary antibody was coupled to protein G magnetic Dynabeads® (Life Technologies) at a ratio of 1 μg antibody per 10 μl beads. Cell lysates were precleared by incubation with Dynabeads without antibody for 30 min at 4 °C. After preclearing, cell lysates were incubated with coupled antibody overnight at 4 °C. Immune complexes were washed three times in lysis buffer, heated 10 min at 75 °C, centrifugated 2 min at 14,000 rpm at 4 °C and resolved on a 4–12% NuPage gradient gel. Gels were stained with Coomassie Brilliant Blue (Thermo Scientific) overnight at room temperature and destained for several hours. Protein bands were excised and washed with water, followed by 50% acetonitrile and acetonitrile before vacuum drying. For in-gel protein digestion 0.1 μg of trypsin in digestion solution (50 mM NH_4HCO_3 in 10% acetonitrile) was added to each gel band. Digestion proceeded overnight at 37 °C, after which the generated peptide mixture was acidified with formic acid. These peptide mixtures were analyzed by liquid chromatography mass spectrometry (LC–MS/MS) using a LTQ Orbitrap XL mass spectrometer (Thermo Scientific). For phosphopeptide enrichment TiO_2 Mag Sepharose beads (GE Healthcare) were used according to the manufacturer's instructions, prior to LC–MS/MS analysis.

2.6. ELISA

Plates (Nunc Maxisorp for 3,3′,5,5′-tetramethylbenzidine (TMB)-based detection or Costar 96, half area black polystyrene for Quantablue© (Thermo Scientific) detection) were coated overnight at 4 °C with capturing antibody (anti-GFP or anti-LRRK2) in 10 mM Tris pH 8.5, 10 mM NaCl, 10 mM NaN_3. After five washes in PBST (phosphate buffered saline with 0.05% (v/v) Tween-20) plates were blocked in 0.1% casein and samples, diluted in blocking buffer with added protease and phosphatase inhibitors, were applied on the plate and incubated for at least 1 h at 4 °C. Primary antibodies were added and plates were kept overnight at 4 °C followed by five washes in PBST, secondary HRP-labeled antibody incubation for 1 h and another 5 washes in PBST. Detection was performed with colorimetric ($A_{450\,nm}$) detection of HRP activity with TMB as a substrate or with fluorescent detection *via* Quantablue methodology according to the manufacturer's instructions (Thermo Scientific).

3. Results

3.1. Identification of GFP-LRRK2 phosphorylation sites in HEK293 cells

For overexpression of GFP-tagged LRRK2 (wildtype (WT), G2019S or D1994A) in HEK293 cells, we used BacMam technology (Life Technologies). To evaluate and optimize the efficiency of this technique the transduction was tested at several multiplicities of infection (MOI), *i.e.* 10, 30 and 50. Western blot analysis revealed that at MOI 30 LRRK2 expression is at its maximum level (Fig. 1A). Therefore, it was decided to use this MOI in further experiments.

To verify which sites on the LRRK2 variants are phosphorylated, we purified overexpressed GFP-LRRK2 proteins (WT, G2019S and D1994A). Use of the kinase deficient D1994A LRRK2 would allow to estimate kinase-dependency of an observed phosphosite. From lysates of HEK293 cells transfected with different GFP-LRRK2 variants, GFP-LRRK2 proteins were isolated *via* immunoprecipitation with an anti-GFP antibody. Eluted proteins were resolved *via* electrophoresis and the gels were stained with Coomassie Brilliant Blue (Fig. 1B). LC–MS/MS was used to analyze the presence of phosphorylation sites on LRRK2. Fig. 1D shows the peptide sequences in which phosphorylated residues were detected, with an example of an MS/MS spectrum for S910 in Fig. 1E. Several residues that are phosphorylated in the presence of WT and G2019S, but not D1994A LRRK2 are identified by LC–MS/MS (Fig. 1C). These sites also included S910 and S935 which is in correspondence with earlier work [10].

3.2. Monitoring S910 and S935 GFP-LRRK2 phosphorylation with western blotting

To obtain further evidence that LRRK2 has a role in the phosphorylation of its own S910 and S935 sites, we overexpressed wildtype, G2019S and D1994A GFP-LRRK2 in HEK293 cells *via* Lipofectamine transfection. One day after transfection cells were treated with 0.1% DMSO or 10 μM LRRK2-IN-1 [13] for 1 h. We measured levels of pS910 and pS935 GFP-LRRK2 phosphorylation *via* western blotting using phosphospecific antibodies (Fig. 2A). When treated with DMSO, comparison of phosphorylation levels indicates that phosphorylation of both S910 and S935 is unaltered in cells expressing G2019S GFP-LRRK2, but significantly downregulated in cells expressing D1994A GFP-LRRK2 ($p < 0.01$), when compared to wildtype GFP-LRRK2 expressing cells (Fig. 2B and C). Treatment with LRRK2-IN-1 significantly decreases phosphorylation of S910 and S935 in cells overexpressing wildtype or G2019S GFP-LRRK2 ($p < 0.01$), but does not significantly affect phosphorylation ($p > 0.05$) in D1994A GFP-LRRK2 overexpressing cells (Fig. 2B and C).

3.3. Detection of overexpressed GFP-LRRK2 with ELISA

A goal of this study is to develop a high-throughput assay for monitoring cellular LRRK2 kinase activity. Given the fact that GFP-tagged LRRK2 displays kinase-dependent signals with anti-pS910

C

Site	WT	G2019S	D1994A
S910	x	x	
S935	x	x	
S955	x	x	
S973	x	x	
S976	x	x	

D

Site	Sequence	Start	End
S910	SN(pS)ISVGEFYR	908	918
S935	HSN(pS)LGPIFDHEDLLK	932	947
S955	ILS(pS)DDSLR	952	960
S973	HSD(pS)ISSLASER	970	981
S976	HSD(pS)IS(pS)LASER	970	981

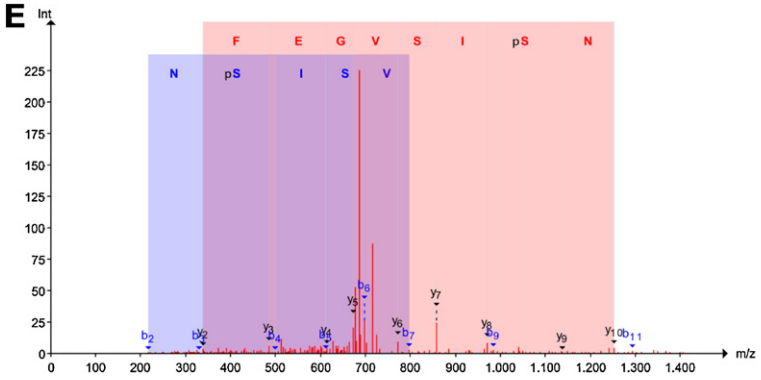

Fig. 1. Identification of GFP-LRRK2 phosphorylation sites in HEK293 cells. (A) HEK293 cells were transduced with BacMam GFP-WT LRRK2 at different MOIs and a LRRK2 blot was used to show expression. MOI 30 was used for further experiments. (B) GFP-LRRK2 was immunoprecipitated with anti-GFP antibody from HEK293 cells. Immunoprecipitates were subjected to electrophoresis and stained with Coomassie Brilliant Blue. (C) Peptide digests of Coomassie Brilliant Blue stained gel bands from WT, G2019S and D1994A LRRK2 were analyzed by LC–MS/MS for the presence of phosphorylated residues. Identified residues are summarized in (C), with an overview of the specific peptide sequences that were detected in (D). Start and end indicate the position of the first and last amino acid, respectively, in the full length protein. (E) Example of MS spectrum for pS910.

and anti-pS935 antibodies, the most straightforward assay is a sandwich ELISA where an anti-GFP antibody is used to capture the overexpressed GFP-LRRK2 followed by detection of total LRRK2 and S935/S910 phosphorylated LRRK2 with the antibodies mentioned above (Fig. 3A). Loading of increasing amounts of total cellular extract from GFP-LRRK2 transduced cells (both WT and D1994A) increases the signal of total LRRK2 (Fig. 3B) with a detection limit below 3 μg of cellular extract. Lysates of cells transduced with untagged LRRK2 or with GFP alone are not giving any appreciable signals, demonstrating the specificity of the sandwich ELISA. Detection with phosphospecific antibodies anti-pS910 and anti-pS935 also shows increased signal in lysates from WT GFP-LRRK2 cells when compared to cells transduced with GFP or untagged LRRK2 (Fig. 3C and D). In contrast, while total LRRK2 levels were prominent, both phospho-specific antibodies failed to detect a signal on GFP-LRRK2 with the D1994A mutation. This again demonstrates that cellular phosphorylation of pS910 and pS935 mainly depends on direct or indirect LRRK2 kinase activity which is in correspondence with work from Nichols et al. [10].

Next, we aimed to optimize the assay to a format where cells, plated and transduced in a 96-well plate, can be lysed with RIPA and subsequently transferred to the assay plate without the need for quantifying protein. As phosphorylation at S935 gives higher signal to noise ratios in comparison to S910, only pS935 and total LRRK2 detection were considered. HEK293 cells were transduced with GFP-LRRK2 in suspension and plated at different densities in a 96-well plate. Twenty-four hours after transfection, medium was aspirated and cells were immediately lysed and frozen. After thawing on ice, one third of the material was analyzed with different parameters as indicated in Fig. 4A. ELISA data clearly show increasing signals in function of cell number. The number of cells indicated in the graph reflects the amount per well and not the amount analyzed (which is 3 times less). According to that, it was concluded that plating 30,000 cells per well is suitable for analyzing both parameters (total and phosphorylated LRRK2) in the ELISA. Validation of the concept and protocol was shown by the 80–90% reduction in pS935/total LRRK2 ratio when D1994A LRRK2 was used instead of WT LRRK2 (Fig. 4B). Pharmacological inhibition of cellular LRRK2 kinase activity was established by treatment of WT LRRK2 transduced cells with increasing concentrations of LRRK2-IN-1. Data in Fig. 4C clearly show a concentration dependent inhibition of LRRK2 at sub-micromolar range of the inhibitor. The same effect was shown on western blot (Fig. 4D). From the data shown in Fig. 4, we suggest that the ELISA procedure is suitable to show a cellular effect of a LRRK2 inhibitor on overexpressed BacMam GFP-LRRK2.

3.4. Effect of LRRK2 mutants on cellular pS935 levels

Next, we verified whether mutations in LRRK2 would affect the cellular pS935 level. Western blots in Fig. 5A show the expression and pS935 level of different mutants of GFP-tagged LRRK2 overexpressed by the use of Lipofectamine transfection. ELISA data in Fig. 5B show no difference between WT and the clinical G2019S mutant ($p > 0.05$). On the other hand, a significant reduction can be observed in the other pathogenic mutant R1441C ($p < 0.001$).

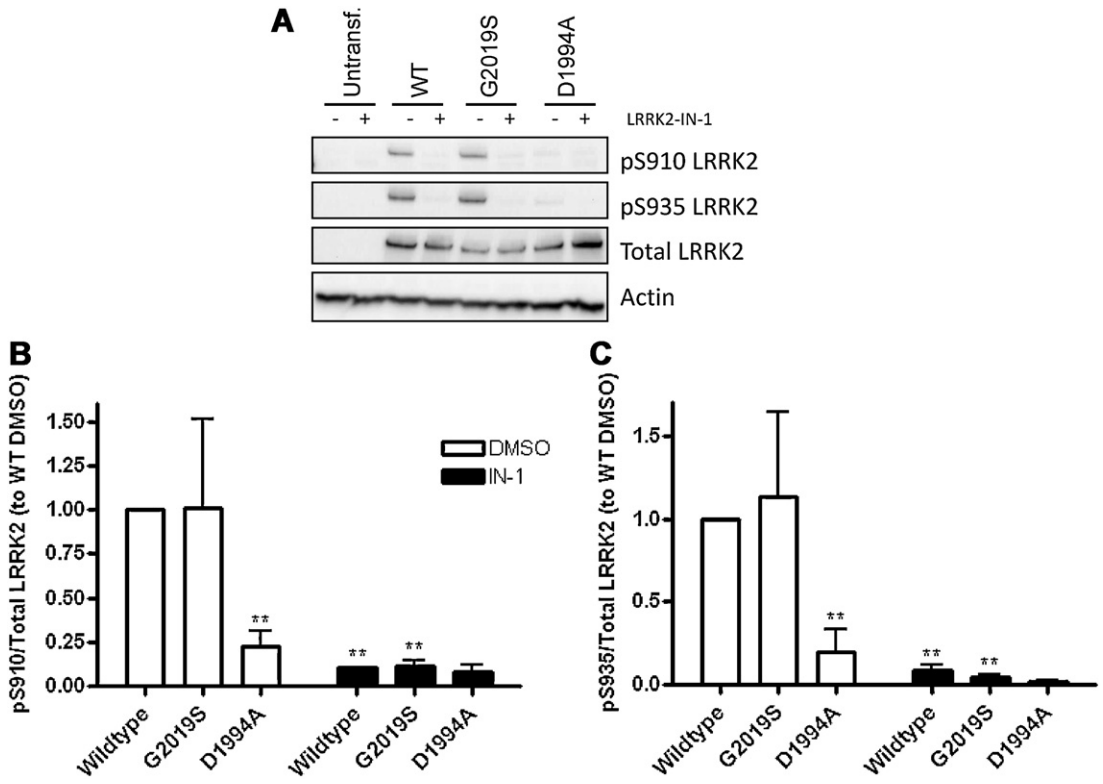

Fig. 2. Monitoring S910 and S935 GFP-LRRK2 phosphorylation with western blotting. (A) Equal amounts of cell lysate from untransfected HEK293 cells or HEK293 cells transfected with WT, G2019S or D1994A LRRK2, treated with 0.1% DMSO as a control or 10 μM LRRK2-IN-1, were subjected to western blot analysis with anti-pS910, pS935 or total LRRK2 antibodies while actin was detected as loading control. The blots are representative of at least 3 experiments (**$p < 0.01$). Ratios of LRRK2 phosphorylated at S910 (B) and S935 (C) to total LRRK2 were calculated and normalized to the ratio in WT LRRK2. Values represent means ± SD ($n = 3$).

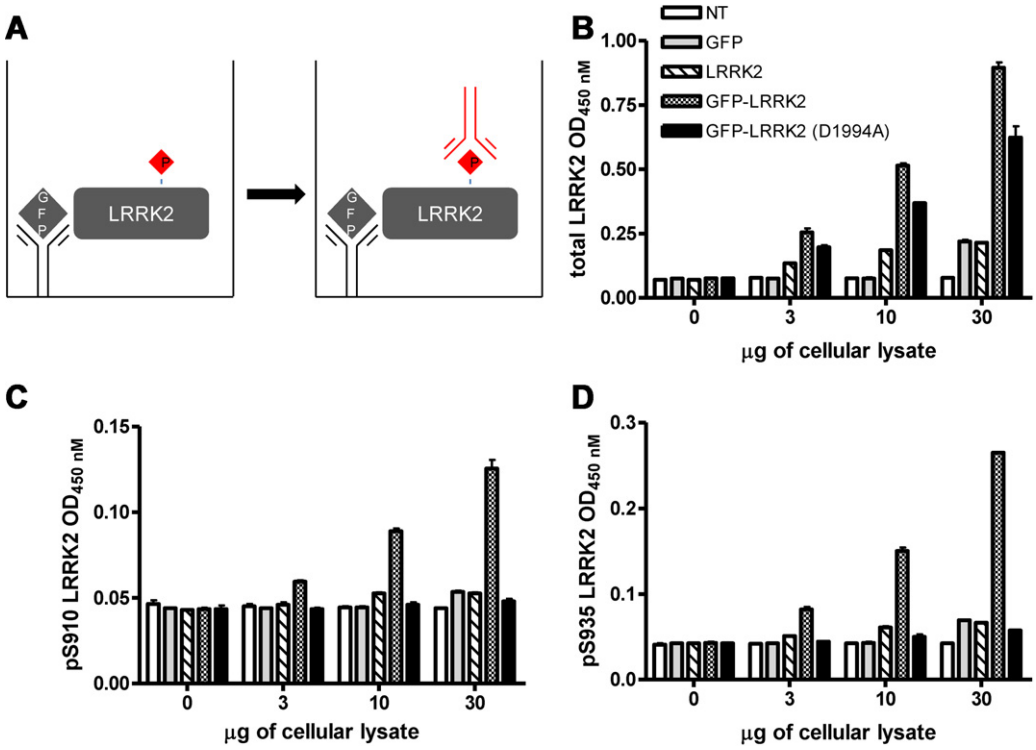

Fig. 3. Detection of GFP-LRRK2 with ELISA. Different amounts of lysates of GFP-LRRK2 (WT or D1994A) transduced HEK293 cells were applied on an ELISA plate with an anti-GFP antibody as indicated in (A) and the captured GFP-LRRK2 was detected with total (B), pS910 (C) or pS935 (D) antibodies with colorimetric measurement as described in Section 2.6. Graphs represent mean OD values ± SD of a representative experiment. Lysates from non-transfected cells (NT), cells transfected with GFP (GFP) or cells transfected with untagged LRRK2 were used as negative controls. Staining with total LRRK2 was positive for WT and D1994A LRRK2 while phospho-specific antibodies were only detecting WT LRRK2.

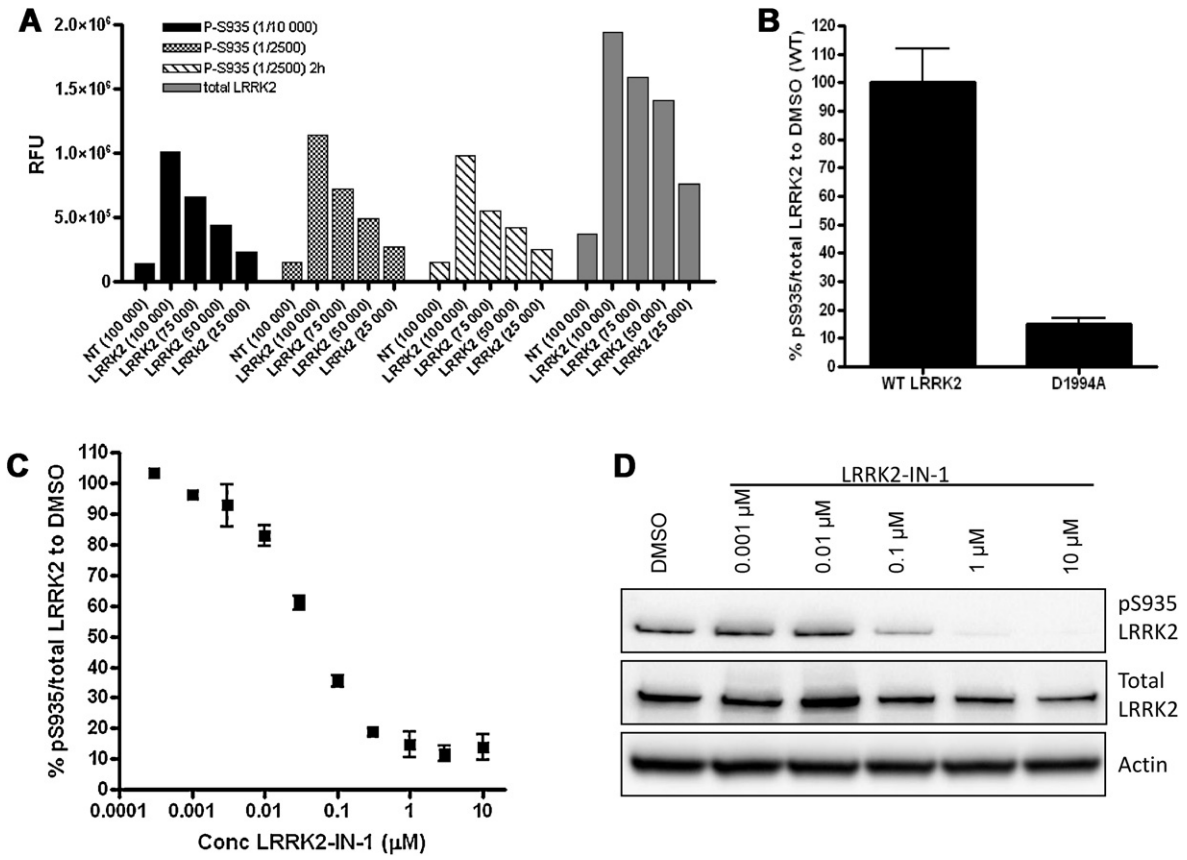

Fig. 4. Detection of GFP-LRRK2 with ELISA. HEK293 cells were transduced in suspension with BacMam GFP-LRRK2 (WT) and plated in a 96-well plate according to indicated cell densities (cells per well). After 24 h cells were lysed in RIPA and one third of the material was analyzed with ELISA using capturing with anti-GFP antibody and detection as indicated in (A). Data are raw signals of a representative experiment. (B) HEK293 cells were transduced with BacMam GFP-LRRK2 (WT or D1994A) and plated in a 96-well plate at a density of 3×10^4 cells per well. pS935/total LRRK2 ratio of cells transduced with WT or D1994A GFP-LRRK2 were determined. (C) Effect of a 1 h treatment with increasing concentrations of LRRK2-IN-1 on pS935/total LRRK2 ratio in WT GFP-LRRK2. For B and C, ratios are normalized to DMSO treated cells transduced with WT GFP-LRRK2. Data are mean ± SD of at least three independent experiments. (D) Equal amounts of cell lysate from HEK293 cells transfected with WT LRRK2 treated with 0.1% DMSO as a control or increasing concentrations of LRRK2-IN-1 were subjected to western blot analysis with anti-pS935 or total LRRK2 antibodies while actin was used as a loading control.

As expected, pS935 levels are strongly reduced in the kinase deficient D1994A variant of LRRK2 ($p < 0.001$) while the kinase inhibitor insensitive variant A2016T [14] shows an inhibition similar to the R1441C mutant ($p < 0.001$).

As phosphorylation of LRRK2 at S935 can be mediated by other kinases, it was determined whether A2016T LRRK2 is differentially affected by LRRK2-IN-1 compared to WT LRRK2. In correspondence to WT GFP-LRRK2 transduced with BacMam, the concentration-dependent inhibition of the compound on protein transfected with Lipofectamine is similar to the BacMam LRRK2 (Fig. 5C). Contrary to WT LRRK2 almost no effect is observed on A2016T LRRK2, showing that LRRK2-IN-1 diminishes LRRK2 pS935 levels by inhibiting LRRK2 kinase activity.

3.5. Detection of endogenous total and pS935 LRRK2 in rodent tissues

Besides determination of cellular LRRK2 kinase activity for compound screening or pathway analysis, detection of endogenous LRRK2 levels and activity in tissue is of interest as a pharmacodynamic readout. First, different tissue samples from WT and LRRK2 knockout (KO) rats were analyzed by immunoprecipitation combined with western blot detection using the MJFF2 antibody (Epitomics). While all of the selected tissues derived from WT rats show appreciable levels of LRRK2 in the immunoprecipitate, no signal is observed in tissues derived from LRRK2 KO rats. Interestingly, aside from the 286 kDa total form of LRRK2 a truncated form of LRRK2 is detected at approximately 196 kDa in wildtype kidney, which is not phosphorylated at S935 (Fig. 6). This unphosphorylated truncated from was also detected in wildtype spleen, but was absent in lung tissue (data not shown). The presence of a truncated form of LRRK2 in kidney tissue was previously described by Herzig et al. [15]. The absence of signal in the tissue samples from LRRK2 KO rats demonstrates specificity of the observed signal. Further, these results indicate that the antibody used for immunoprecipitation seems to be suitable for capturing endogenous LRRK2. Therefore, it was used as a capturing antibody in the ELISA assay as described in Section 2.6 of this paper. From Fig. 6B and C it is clear that in spleen and lung the highest LRRK2 protein levels could be measured, but also in brain and kidney signals were substantial. In none of the tissue samples from LRRK2 KO rats a significant signal could be observed, demonstrating that total and pS935 signals are depending on LRRK2 protein. These data demonstrate that the proposed ELISA can be used for detection of total and pS935 LRRK2 *ex vivo*. In brain and lung pS935 to total LRRK2 ratios appeared to be the highest (Fig. 6D).

As for cellular phosphorylation, we determined whether LRRK2 pS935 levels were altered in brain of R1441G LRRK2 Tg mouse. Data in Fig. 6E indeed confirm a decreased phosphorylation level in R1441G LRRK2 Tg mice compared to WT LRRK2 (Tg and NT) mice.

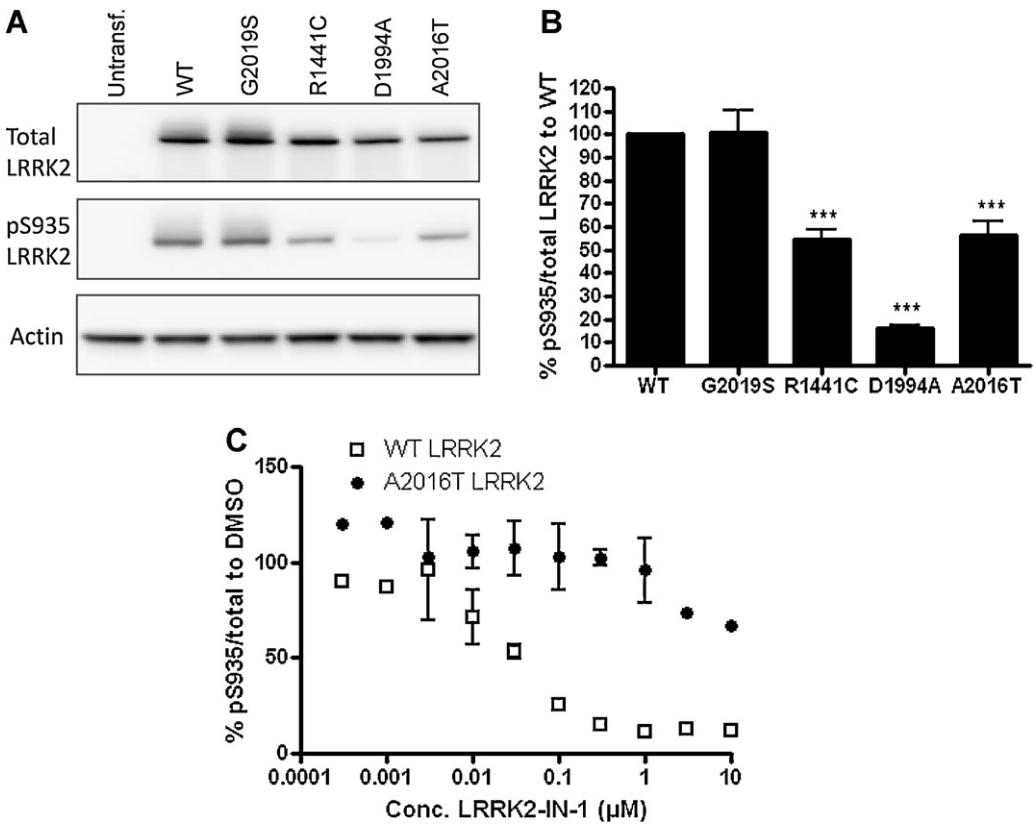

Fig. 5. Effect of LRRK2 mutants on pS935 levels. HEK293 cells were transiently transfected with GFP-tagged LRRK2 constructs mutated at the indicated sites. In (A) representative immunoblots using pS935 and total LRRK2 are shown while in (B) an ELISA is used to determine the pS935/total LRRK2 ratio. Data are mean ± SD of at least three independent experiments (***$p < 0.001$). In (C) the effect of a concentration response curve of the LRRK2-IN-1 compound on WT or A2016T GFP-LRRK2 is shown. The ratios are normalized to the respective DMSO controls.

3.6. Effect of LRRK2 kinase inhibitors on pS935 levels

In the previous section, it was demonstrated that endogenous LRRK2 expression and activity in rodent tissue can be determined by the sandwich ELISA using mouse anti-LRRK2 as capturing antibody and rabbit anti total or phospho S935 LRRK2 as detection antibody. Next, we evaluated whether the assay is a suitable platform to determine pharmacological inhibition of LRRK2 kinase activity. Kidney, spleen and brain tissue from WT mice, treated with NMP/PEG or different concentrations of the brain penetrable LRRK2 inhibitor HG-10-102-01 [12] for 1 h, were analyzed with the ELISA. A dose dependent decrease in pS935/total LRRK2 ratios is observed in all tissues (Fig. 7A). These results are in accordance with immunoblot data (Fig. 7B). As LRRK2 is expressed in human PBMC [13], the pS935 ELISA might also be useful to determine pharmacological inhibition of LRRK2 in human blood. To determine whether the assay is indeed suitable for the analysis of human endogenous LRRK2 activity, PBMC isolated from healthy donors were treated with 0.1% DMSO or 1 μM LRRK2-IN-1 for 1 h. Lysates were analyzed with ELISA, using anti-LRRK2 antibody for capturing and pS935 and total LRRK2 antibodies for detection. Data in Fig. 8 show that LRRK2 protein can be detected in PBMC. Further, treatment of PBMC with LRRK2-IN-1 significantly decreases the pS935 level to less than 30% of the level measured in control cells ($p < 0.01$).

These results clearly demonstrate that pharmacological modulation of LRRK2 can be analyzed accurately with the current assay.

Collectively, data shown in this manuscript demonstrate that pS935 phosphorylation is a good readout to show cellular and *in vivo* LRRK2 activity. The ELISA platform makes it useful for high throughput purposes.

4. Discussion

After the initial discovery of a causal role for LRRK2 mutations in PD, further research in this area has been struggling for years because of the lack of tools to measure LRRK2 expression and kinase activity in cells and tissue. One of the first papers, dedicated to the use of LRRK2 antibodies for western blotting [16], was indicative of the lack of antibodies suitable for endogenous LRRK2 detection in tissue. An even larger issue was the poor insight into the biochemical properties of this large protein, which encompasses several protein–protein interaction domains and two catalytic domains [17–19]. Despite these obstacles, the therapeutic potential of LRRK2 kinase inhibition has been extensively explored [10,20]. This strategy is supported by different sources of evidence showing that increased kinase activity plays a crucial role in the toxic mechanism driven by PD-associated LRRK2 mutations [18,21,22].

Since a few years the first antibodies suitable for detection of endogenous LRRK2 in brain tissue are available (Epitomics, MJFF). In addition, increasing insight has been gained about LRRK2 autophosphorylation and, in light of the limited information of genuine LRRK2 substrates, identification of autophosphorylation sites was a logic approach to develop a marker for LRRK2 activity *in vitro*, in cells and in tissue. In this respect, different sites and corresponding antibodies have been identified and developed respectively. Among these are two antibodies directed against pS910 and pS935 LRRK2. Although these sites are not considered genuine autophosphorylation sites, inhibition of LRRK2 kinase activity has been shown to downregulate their phosphorylation [14,23]. This suggests that LRRK2 activity does have a role in S910 and S935 phosphorylation, possibly through the regulation of a feedback pathway including

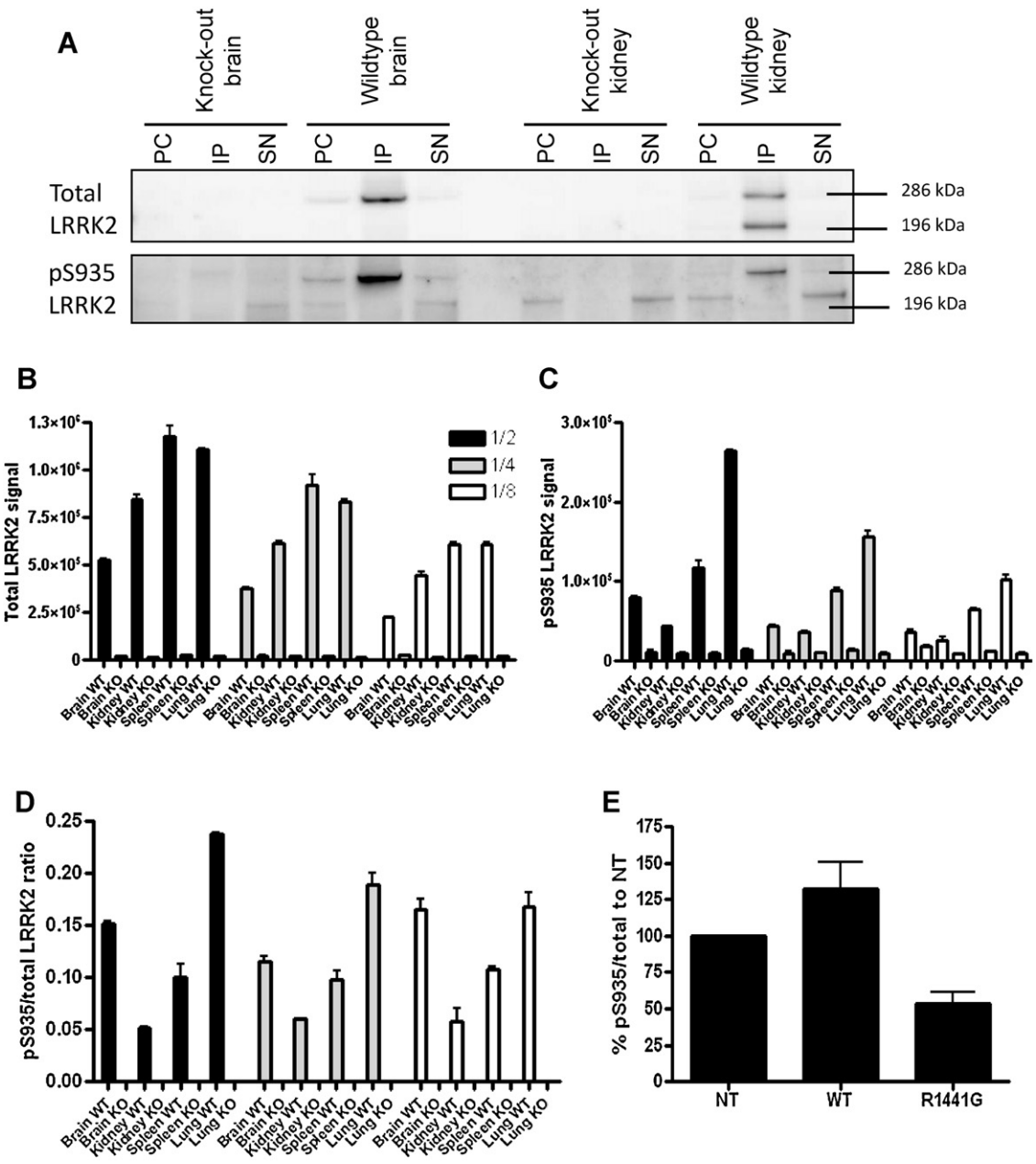

Fig. 6. Detection of endogenous LRRK2 in rodent tissue. Brain and kidney homogenates of WT and LRRK2 KO rats were subjected to immunoprecipitation to isolate LRRK2. Preclear material (PC), immunoprecipitates (IP) and supernatant after IP (SN) were subjected to western blot analysis with anti-pS935 or total LRRK2 antibodies. Different dilutions of brain, kidney, spleen and lung total protein extracts (5 μg/μl) derived from WT or LRRK2 KO rats were analyzed with ELISA using anti-LRRK2 for capturing and (B) anti-total LRRK2 or (C) anti-pS935 LRRK2 as detection antibody. (D) From each sample the pS935/total LRRK2 ratio is calculated and data are mean ± SD from at least 3 biological replicates. (E) LRRK2 protein and pS935 levels in mouse brain lysates from non-transgenic (NT), LRRK2 transgenic (Tg) or R1441G LRRK2 (R1441G) transgenic mice are determined with ELISA and normalized to pS935/total LRRK2 ratio in non-transgenic (NT) animals. Data are mean ± SD from at least 3 biological replicates (*$p < 0.05$, to NT).

other kinases, as suggested by other reports. Therefore, the antibodies directed against pS910 and pS935 LRRK2 are very useful tools for measurement of cellular activity of overexpressed LRRK2 [10].

In this study a high-throughput ELISA has been established to measure cellular pS935 LRRK2 levels in a 96-well format. BacMam-mediated transduction of GFP-LRRK2 in HEK293 cells resulted in highly expressed protein that was phosphorylated at several residues, including S910 and S935 (Fig. 1). The fact that phosphopeptides were not found in the kinase-deficient variant D1994A GFP-LRRK2 was indicative of kinase dependency of the phosphorylation events, which is in correspondence with other work [10]. Accordingly, similar phosphorylation levels were measured on western blot using pS910 and pS935 antibodies (Fig. 2B and C). For further development into an ELISA we used the GFP-tag to capture overexpressed LRRK2 by use of an anti-GFP antibody (Fig. 3A). In a lysate of HEK293 cells transduced with BacMam GFP-LRRK2, this assay can detect pS935 and total LRRK2 in amounts of total cellular extract below 10 μg (Fig. 3B–D). Alternatively, cells can be transduced and plated in a 96-well plate (Fig. 4A). In that case, plating of 30,000 BacMam transduced cells per well is sufficient to demonstrate a concentration-dependent effect of the LRRK2-IN-1 inhibitor (Fig. 4C). This compound was first published by Deng et al. [13] and was shown to inhibit LRRK2 kinase activity at nanomolar concentrations *in vitro*. In cellular assays inhibition occurred at submicromolar concentrations of LRRK2-IN-1, which is consistent with our findings in the ELISA.

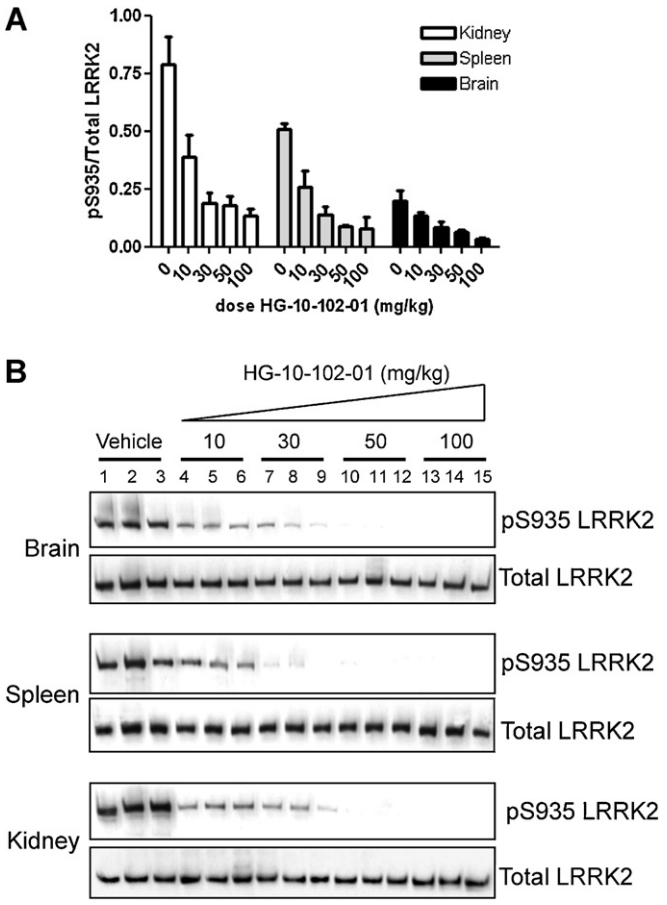

Fig. 7. Effect of LRRK2 inhibitor HG-10-102-01 on LRRK2 S935 phosphorylation. Pharmacodynamic study of HG-10-102-01 from brain, spleen and kidney following intraperitoneal administration of the indicated doses. (A) Homogenates were analyzed with ELISA using anti-LRRK2 antibody for capturing and total LRRK2 and pS935 LRRK2 antibodies for detection. Data are mean ± SD of at least three independent experiments. (B) Equal amounts of tissue homogenate were subjected to western blot analysis with pS935 or total LRRK2 antibodies.

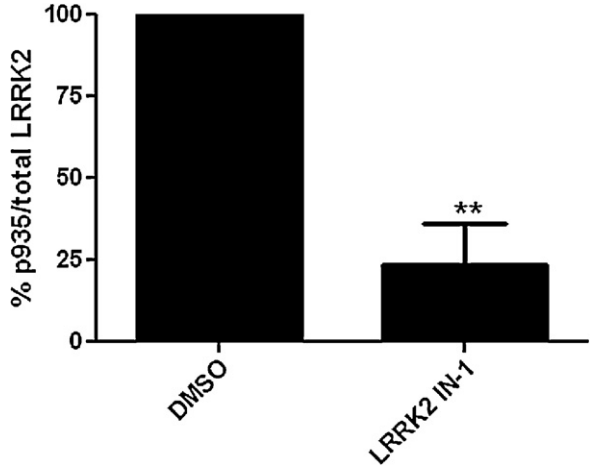

Fig. 8. Detection of endogenous LRRK2 in PBMCs from healthy donors. Lysates of PBMCs treated with 0.1% DMSO or 1 μM LRRK2-IN-1 for 1 h, were analyzed with ELISA using anti-LRRK2 antibody for capturing and total LRRK2 and PhosphoS935 LRRK2 antibodies for detection. pS935/total LRRK2 ratios were determined and normalized to DMSO treated cells. Data are mean ± SD of at least three independent experiments (**$p < 0.01$).

LRRK2 phosphorylation at S910 and S935 has been implicated in 14-3-3 chaperone binding to maintain cytoplasmic localization of LRRK2 [11]. Although different kinases (*e.g.* PKA and IKKB) have been reported to mediate these phosphorylations [24,25], measurement of S935 phosphorylation is a good readout for cellular LRRK2 kinase activity. Indeed, expression of drug resistant A2016T LRRK2 [13] prevents the inhibition by LRRK2-IN-1 (Fig. 5C). Like the PD-associated mutation R1441C, this mutant shows reduced S935 phosphorylation in comparison to WT LRRK2 (Fig. 5A and B). Use of less specific inhibitors also reduced phosphorylation in the A2016T mutant (data not shown); suggesting that monitoring pS935 levels in A2016T LRRK2 is useful as counterscreen. The diminished pS935 levels in the R1441C mutant (Fig. 5A and B) are in agreement with other reports [25,26], but the reason for this diminished phosphorylation remains unknown at this point.

Transfer of the assay to a format where LRRK2 is captured by an anti-LRRK2 antibody allowed verifying levels and activity of endogenous LRRK2. To validate this we used different tissues from WT and LRRK2 KO rats. From both western blot and ELISA data (Fig. 6) it is clear that LRRK2 protein and pS935 levels can be measured in brain, kidney, spleen and lung tissue derived from WT rats. This could be performed in tissue samples with a total protein concentration lower than 1 μg/ml. In contrast, in none of the tissue samples from LRRK2 KO rats any substantial signal could be observed, which demonstrates that signals in the ELISA are derived from endogenous LRRK2 protein. The truncated form detected in WT kidney is not phosphorylated at S935 and lowers the relative phosphorylation level. Interestingly, this truncated form is only detected when using the MJFF2 antibody, which recognizes an epitope in leucine-rich repeat region of LRRK2, but not with the anti-LRRK2 antibody provided by Dr. Alessi, which recognizes an epitope near the N-terminal end of LRRK2 (data not shown). This leads us to speculate that in this truncated form a peptide sequence near the N-terminal end of LRRK2 is lacking. The physiological relevance of this truncated form and whether this is the same form as reported by Herzig et al. [15] remains to be elucidated.

The fact that monitoring pS935 is a suitable readout to show target engagement of a compound in PD patient-derived material [13] makes the ELISA an important step in the development of a pharmacodynamic read-out for LRRK2 activity. Our data clearly show that the assay is a good tool for measuring the effect of LRRK2 kinase inhibitors, both in rodent and human samples (Figs. 7 and 8).

As mentioned above, the PD-associated R1441C mutant displayed reduced phosphorylation at S935 when overexpressed in cells. With the ELISA using anti-LRRK2 antibody for capturing, it could be demonstrated that LRRK2 from R1441G Tg mice has a lower pS935/total LRRK2 ratio in comparison to WT Tg LRRK2 but also to NT mice with endogenous mouse LRRK2 (Fig. 6E). Again, the underlying mechanism of this phenomenon is unclear at this point. Decreased kinase activity has not been reported for the R1441C/G mutants, but in some reports it is suggested that this mutation lowers GTPase activity, resulting in an increased GTP binding that could ultimately lead to increased kinase activity [27,28]. While Hermanson et al. detect a slight increase in pS935 levels in G2019S LRRK2 when compared to wildtype LRRK2 measured in a TR-FRET assay [23], the G2019S mutant does not show a significant change in S935 phosphorylation in our hands. At this point it is unclear whether this is a physiological property of G2019S or whether this is due to the high level of S935 phosphorylation in our cellular model. Given the fact that, in our hands, a reduction in phosphorylation is seen in the R1441C/G LRRK2 mutant while the G2019S mutant does not show a significant change in S935 phosphorylation, we conclude that not a reduction or elevation in phosphorylation, but rather an altered phosphorylation status is a general property of PD-associated LRRK2 mutants. This is in accordance with recently

published data in *Drosophila melanogaster*. Studies in *Drosophila* show that both too much and too little endophilin A phosphorylation by LRRK2 impedes synaptic endocytosis [29]. The physiological consequence of this remains to be determined. It also underscores the need to establish assays based on genuine autophosphorylation sites or on substrate phosphorylation sites.

In conclusion, we present two high-throughput assays to monitor cellular and *in vivo* expression and activity of LRRK2. Our data describe an ELISA to measure endogenous LRRK2 expression and pS935 phosphorylation in biological samples, which is essential to develop a pharmacodynamic readout of LRRK2 kinase activity.

Acknowledgements

We thank the MJFF for the coordination of LRRK2 antibody production and validation. We thank members of the Patrik Verstreken, Bart De Strooper and Kris Gevaert laboratories for comments. This work is supported by an IWT-Vlaanderen R&D grant.

References

[1] I. Martin, V.L. Dawson, T.M. Dawson, Recent advances in the genetics of Parkinson's disease, Annu. Rev. Genomics Hum. Genet. 12 (2011) 301–325.
[2] D.G. Healy, M. Falchi, S.S. O'Sullivan, V. Bonifati, A. Durr, S. Bressman, A. Brice, J. Aasly, C.P. Zabetian, S. Goldwurm, Phenotype, genotype, and worldwide genetic penetrance of LRRK2-associated Parkinson's disease: a case–control study, Lancet Neurol. 7 (2008) 583–590.
[3] A. Zimprich, S. Biskup, P. Leitner, P. Lichtner, M. Farrer, S. Lincoln, J. Kachergus, M. Hulihan, R.J. Uitti, D.B. Calne, Mutations in LRRK2 cause autosomal-dominant Parkinsonism with pleomorphic pathology, Neuron 44 (2004) 601–607.
[4] E. Greggio, M.R. Cookson, Leucine-rich repeat kinase 2 mutations and Parkinson's disease: three questions, ASN Neuro 1 (2009) 13–24.
[5] E.K. Tan, R. Peng, Y.Y. Teo, L.C. Tan, D. Angeles, P. Ho, M.L. Chen, C.H. Lin, X.Y. Mao, X.L. Chang, Multiple LRRK2 variants modulate risk of Parkinson disease: a Chinese multicenter study, Hum. Mutat. 31 (2010) 561–568.
[6] S. Kamikawaji, G. Ito, T. Iwatsubo, Identification of the autophosphorylation sites of LRRK2, Biochemistry 48 (2009) 10963–10975.
[7] Y. Imai, S. Gehrke, H.Q. Wang, R. Takahashi, K. Hasegawa, E. Oota, B. Lu, Phosphorylation of 4E-BP by LRRK2 affects the maintenance of dopaminergic neurons in *Drosophila*, EMBO J. 27 (2008) 2432–2443.
[8] E. Ohta, F. Kawakami, M. Kubo, F. Obata, LRRK2 directly phosphorylates Akt1 as a possible physiological substrate: impairment of the kinase activity by Parkinson's disease-associated mutations, FEBS Lett. 585 (2011) 2165–2170.
[9] L. Parisiadou, C. Xie, H.J. Cho, X. Lin, X.L. Gu, C.X. Long, E. Lobbestael, V. Baekelandt, J.M. Taymans, L. Sun, Phosphorylation of ezrin/radixin/moesin proteins by LRRK2 promotes the rearrangement of actin cytoskeleton in neuronal morphogenesis, J. Neurosci. 29 (2009) 13971–13980.
[10] R.J. Nichols, N. Dzamko, N.A. Morrice, D.G. Campbell, M. Deak, A. Ordureau, T. Macartney, Y. Tong, J. Shen, A.R. Prescott, 14-3-3 binding to LRRK2 is disrupted by multiple Parkinson's disease-associated mutations and regulates cytoplasmic localization, Biochem. J. 430 (2010) 393–404.
[11] N. Dzamko, M. Deak, F. Hentati, A.D. Reith, A.R. Prescott, D.R. Alessi, R.J. Nichols, Inhibition of LRRK2 kinase activity leads to dephosphorylation of Ser910/Ser935, disruption of 14-3-3 binding and altered cytoplasmic localisation, Biochem. J. 430 (2010) 405–413.
[12] H.G. Choi, J. Zhang, X. Deng, J.M. Hatcher, M.P. Patricelli, Z. Zhao, D.R. Alessi, N.S. Gray, Brain penetrant LRRK2 inhibitor, ACS Med. Chem. Lett. 3 (2012) 658–662.
[13] X. Deng, N. Dzamko, A. Prescott, P. Davies, Q. Liu, Q. Yang, J.D. Lee, M.P. Patricelli, T.K. Nomanbhoy, D.R. Alessi, Characterization of a selective inhibitor of the Parkinson's disease kinase LRRK2, Nat. Chem. Biol. 7 (2011) 203–205.
[14] R. Nichols, N. Dzamko, J. Hutti, L. Cantley, M. Deak, J. Moran, P. Bamborough, A. Reith, D. Alessi, Substrate specificity and inhibitors of LRRK2, a protein kinase mutated in Parkinson's disease, Biochem. J. 424 (2009) 47–60.
[15] M.C. Herzig, C. Kolly, E. Persohn, D. Theil, T. Schweizer, T. Hafner, C. Stemmelen, T.J. Troxler, P. Schmid, S. Danner, LRRK2 protein levels are determined by kinase function and are crucial for kidney and lung homeostasis in mice, Hum. Mol. Genet. 20 (2011) 4209–4223.
[16] S. Biskup, D. Moore, A. Rea, B. Lorenz-Deperieux, C. Coombes, V. Dawson, T. Dawson, A. West, Dynamic and redundant regulation of LRRK2 and LRRK1 expression, BMC Neurosci. 8 (2007) 102.
[17] X. Li, Y.C. Tan, S. Poulose, C.W. Olanow, X.Y. Huang, Z. Yue, Leucine-rich repeat kinase 2 (LRRK2)/PARK8 possesses GTPase activity that is altered in familial Parkinson's disease R1441C/G mutants, J. Neurochem. 103 (2007) 238–247.
[18] W.W. Smith, Z. Pei, H. Jiang, V.L. Dawson, T.M. Dawson, C.A. Ross, Kinase activity of mutant LRRK2 mediates neuronal toxicity, Nat. Neurosci. 9 (2006) 1231–1233.
[19] A.B. West, D.J. Moore, S. Biskup, A. Bugayenko, W.W. Smith, C.A. Ross, V.L. Dawson, T.M. Dawson, Parkinson's disease-associated mutations in leucine-rich repeat kinase 2 augment kinase activity, Proc. Natl. Acad. Sci. U.S.A. 102 (2005) 16842–16847.
[20] B.D. Lee, J.H. Shin, J. VanKampen, L. Petrucelli, A.B. West, H.S. Ko, Y.I. Lee, K.A. Maguire-Zeiss, W.J. Bowers, H.J. Federoff, Inhibitors of leucine-rich repeat kinase-2 protect against models of Parkinson's disease, Nat. Med. 16 (2010) 998–1000.
[21] E. Greggio, S. Jain, A. Kingsbury, R. Bandopadhyay, P. Lewis, A. Kaganovich, M.P. van der Brug, A. Beilina, J. Blackinton, K.J. Thomas, Kinase activity is required for the toxic effects of mutant LRRK2/dardarin, Neurobiol. Dis. 23 (2006) 329–341.
[22] D. MacLeod, J. Dowman, R. Hammond, T. Leete, K. Inoue, A. Abeliovich, The familial Parkinsonism gene LRRK2 regulates neurite process morphology, Neuron 52 (2006) 587–593.
[23] S.B. Hermanson, C.B. Carlson, S.M. Riddle, J. Zhao, K.W. Vogel, R.J. Nichols, K. Bi, Screening for novel LRRK2 inhibitors using a high-throughput TR-FRET cellular assay for LRRK2 Ser935 phosphorylation, PLoS ONE 7 (2012) e43580.
[24] N. Dzamko, F. Inesta-Vaquera, J. Zhang, C. Xie, H. Cai, S. Arthur, L. Tan, H. Choi, N. Gray, P. Cohen, The IkappaB kinase family phosphorylates the Parkinsonâ€TMs disease kinase LRRK2 at Ser935 and Ser910 during Toll-like receptor signaling, PLoS ONE 7 (2012) e39132.
[25] X. Li, Q.J. Wang, N. Pan, S. Lee, Y. Zhao, B.T. Chait, Z. Yue, Phosphorylation-dependent 14-3-3 binding to LRRK2 is impaired by common mutations of familial Parkinson's disease, PLoS ONE 6 (2011) e17153.
[26] E.A. Doggett, J. Zhao, C.N. Mork, D. Hu, R.J. Nichols, Phosphorylation of LRRK2 serines 955 and 973 is disrupted by Parkinson's disease mutations and LRRK2 pharmacological inhibition, J. Neurochem. 120 (2012) 37–45.
[27] V. Daniëls, R. Vancraenenbroeck, B.M.H. Law, E. Greggio, E. Lobbestael, F. Gao, M. De Maeyer, M.R. Cookson, K. Harvey, V. Baekelandt, Insight into the mode of action of the LRRK2 Y1699C pathogenic mutant, J. Neurochem. 116 (2011) 304–315.
[28] L. Guo, P.N. Gandhi, W. Wang, R.B. Petersen, A.L. Wilson-Delfosse, S.G. Chen, The Parkinson's disease-associated protein, leucine-rich repeat kinase 2 (LRRK2), is an authentic GTPase that stimulates kinase activity, Exp. Cell Res. 313 (2007) 3658–3670.
[29] S. Matta, K. Van Kolen, R. da Cunha, G. van den Bogaart, W. Mandemakers, K. Miskiewicz, P.-J. De Bock, V. Morais, S. Vilain, D. Haddad, L. Delbroek, J. Swerts, L. Chávez-Gutiérrez, G. Esposito, G. Daneels, E. Karran, M. Holt, K. Gevaert, D. Moechars, B. De Strooper, P. Verstreken, LRRK2 controls an EndoA phosphorylation cycle in synaptic endocytosis, Neuron 75 (2012) 1008–1021.